remained negative for λ chains. This phenomenon may be reasonably explained by the fact that IL-13, even when used at high concentrations, had no ability to induce RAG expression. It is possible therefore that the RAG genes are not regulated by IL-13 at any concentrations.

Although the great majority of mature blood B cells expressed surface IL-4Rα, about 30% of the cells were positive for IL-13Rα1. Low levels of IL-13Rα1 expression were also observed on $CD19^+$ cells of PBMC. Although most naive tonsil B cells have been reported to be labeled by the selected anti-IL-13Rα1 [35], our results from the expression studies using mature blood B cells imply a quantitative difference between IL-4Rα- and IL-13Rα1-bearing cells. This difference may reflect the magnitude of the activities of IL-4 and IL-13, as was demonstrated by the finding that IL-4 induced higher expression of AID in blood B cells activated via CD40 than did IL-13. Similarly, CD23 expression has been shown to be enhanced more potently by IL-4 than by IL-13 [36]. Our observation that IL-4, but not IL-13, was effective in inducing RAG expression further suggests that the γc could be involved in the induction of RAG expression leading to light chain replacement. This suggestion is supported by a previous report describing that IL-7, which uses γc for optimal signal transduction, was able to induce RAG expression in mouse spleen B cells activated via CD40 [23]. Under the same experimental conditions, however, other cytokines, such as IL-5, IL-6, and IL-10, were ineffective for RAG expression. Observations made with mouse B cells indicate the participation of the γc in the induction of RAG expression. Collectively, RAG expression by mature B cells is critically dependent on activation of γc and CD40.

We found that RAG expression combined with AID and IgE expression by IL-4 plus anti-CD40-stimulated blood B cells allowed light chain replacement in the induced IgE^+ cells. Thus, RAG-dependent replacement appears to precede IgE expression. Similar RAG expression combined with IgG1 expression has been found in mouse spleen B cells after IL-4 plus LPS stimulation [22]. These findings are in keeping with recent evidence analyzing human tonsil B cell subsets, in which coexpression of RAG and total IgG transcripts was detectable in postswitch memory cells of the germinal center [28]. Although blood B cells activated via CD40 responded to both IL-4 and IL-13 with AID and IgE expression, the de novo synthesis of λ chains by purified κ^+ cells was induced in parallel with IL-4-dependent RAG expression. This light chain replacement was detected in a population of IgE^+ cells. Thus, some of postswitch IgE-expressing cells induced in response to IL-4 bear newly rearranged λ chains, which may alter affinity of IgE due to revision of original antigen receptors. Similar alternations in affinity have been found in other isotypes [21,34]. These findings imply that IL-4-dependent RAG expression and subsequent light chain gene rearrangement in mature B cells may contribute to affinity maturation of IgE antibodies.

In summary, we have shown that IL-4, but not IL-13, is effective in inducing RAG-1 and RAG-2 expression in mature human blood B cells activated via CD40. In addition, IL-4-dependent RAG expression combined with AID and IgE expression allows some of the κ^+ cells switched to IgE to express newly rearranged λ chains. These findings indicate that IL-4-responsive cells, unlike IL-13-responsive cells, undergo receptor revision in parallel with RAG expression and suggest that IL-4-dependent receptor revision may contribute to the regulation of affinity maturation of IgE antibodies.

Acknowledgments

This work was supported in part by a grant from the Japanese Ministry of Health, Labor, and Welfare.

References

[1] G. Zurawski, J.E. de Vries, Interleukin 13, an interleukin 4-like cytokine that acts on monocytes and B cells, but not on T cells, Immunol. Today 15 (1994) 19–26.
[2] P. Chomarat, J. Banchereau, Interleukin-4 and interleukin-13: their similarities and discrepancies, Int. Rev. Immunol. 17 (1998) 1–52.
[3] G.J. McKenzie, P.G. Fallon, C.L. Emson, R.K. Grencis, A.N. McKenzie, Simultaneous disruption of interleukin (IL)-4 and IL-13 defines individual roles in T helper cell type 2-mediated responses, J. Exp. Med. 189 (1999) 1565–1572.
[4] J.F. Gauchat, D.A. Lebman, R.J. Coffman, H. Gascan, J.E. de Vries, Structure and expression of germline ε transcripts in human B cells induced by interleukin 4 to switch to IgE production, J. Exp. Med. 172 (1990) 463–473.
[5] J. Punnonen, G. Aversa, B.G. Cocks, A.N. McKenzie, S. Menon, G. Zurawski, R. de Waal Malefyt, J.E. de Vries, Interleukin 13 induces interleukin 4-independent IgG4 and IgE synthesis and CD23 expression by human B cells, Proc. Natl. Acad. Sci. USA 90 (1993) 3730–3734.
[6] M. Kondo, T. Takeshita, N. Ishii, M. Nakamura, S. Watanabe, K. Arai, K. Sugamura, Sharing of the interleukin-2 (IL-2) receptor γ chain between receptors for IL-2 and IL-4, Science 262 (1993) 1874–1877.
[7] D.J. Hilton, J.G. Zhang, D. Metcalf, W.S. Alexander, N.A. Nicola, T.A. Willson, Cloning and characterization of a binding subunit of the interleukin 13 receptor that is also a component of the interleukin 4 receptor, Proc. Natl. Acad. Sci. USA 93 (1996) 497–501.
[8] J.F. Gauchat, E. Schlagenhauf, N.P. Feng, R. Moser, M. Yamage, P. Jeannin, S. Alouani, G. Elson, L.D. Notarangelo, T. Wells, E.P. Eugster, J.Y. Bonnefoy, A novel 4-kb interleukin-13 receptor α mRNA expressed in human B, T, and endothelial cells encoding an alternate type-II-interleukin-4/interleukin-13 receptor, Eur. J. Immunol. 27 (1997) 971–978.
[9] D.D. Donaldson, M.J. Whitters, L.J. Fitz, T.Y. Neben, H. Finnerty, S.L. Henderson, R.M. O'Hara Jr., D.R. Beier, K.J. Turner, C.R. Wood, M. Collins, The murine IL-13 receptor α2: molecular cloning, characterization, and comparison with murine IL-13 receptor α1, J. Immunol. 161 (1998) 2317–2324.
[10] K. Kawakami, J. Taguchi, T. Murata, R.K. Puri, The interleukin-13 receptor α2 chain: an essential component for binding and

internalization but not for interleukin-13-induced signal transduction through the STAT6 pathway, Blood 97 (2001) 2673–2679.
[11] A.D. Keegan, K. Nelms, M. White, L.M. Wang, J.H. Pierce, W.E. Paul, An IL-4 receptor region containing an insulin receptor motif is important for IL-4-mediated IRS-1 phosphorylation and cell growth, Cell 76 (1994) 811–820.
[12] J.N. Ihle, Cytokine receptor signalling, Nature 377 (1995) 591–594.
[13] W.J. Leonard, J.J. O'Shea, Jaks and STATs: biological implications, Annu. Rev. Immunol. 16 (1998) 293–322.
[14] K. Ikizawa, Y. Yanagihara, Possible involvement of Shc in IL-4-induced germline ε transcription in a human B cell line, Biochem. Biophys. Res. Commun. 268 (2000) 54–59.
[15] R. Umeshita-Suyama, R. Sugimoto, M. Akaiwa, K. Arima, B. Yu, M. Wada, M. Kuwan, K. Nakajima, N. Hamasaki, K. Izuhara, Characterization of IL-4 and IL-13 signals dependent on the human IL-13 receptor α chain 1: redundancy of requirement of tyrosine residue for STAT3 activation, Int. Immunol. 12 (2000) 1499–1509.
[16] L.B. Bacharier, H. Jabara, R.S. Geha, Molecular mechanisms of immunoglobulin E regulation, Int. Arch. Allergy Immunol. 115 (1998) 257–269.
[17] M. Muramatsu, K. Kinoshita, S. Fagarasan, S. Yamada, Y. Shinkai, T. Honjo, Class switch recombination and somatic hypermutation require activation-induced cytidine deaminase (AID), a potent RNA editing enzyme, Cell 102 (2000) 553–563.
[18] R. Revy, T. Muto, Y. Levy, F. Geissman, A. Plebani, O. Sanal, N. Catalan, M. Forveile, R. Dufourcq-Lagelouse, A. Gennery, I. Tezcan, F. Ersoy, H. Kayserili, A.G. Ugazio, N. Brousse, M. Muramatsu, L.D. Notarangelo, K. Kinoshita, T. Honjo, A. Fischer, A. Durandy, Activation-induced cytidine deaminase (AID) deficiency causes the autosomal recessive form of the hyper-IgM syndrome (HIGM2), Cell 102 (2000) 565–575.
[19] K.F. Chua, F.W. Alt, J.P. Manis, The function of AID in somatic mutation and class switch recombination: upstream or downstream of DNA breaks, J. Exp. Med. 195 (2002) F37–F41.
[20] M. Hikida, M. Mori, T. Takai, K. Tomochika, K. Hamatani, H. Ohmori, Reexpression of RAG-1 and RAG-2 genes in activated mature mouse B cells, Science 274 (1996) 2092–2094.
[21] F. Papavasiliou, R. Casellas, H. Suh, X.-F. Qin, E. Besmer, R. Pelanda, D. Nemazee, K. Rajewsky, M.C. Nessenzweig, V(D)J recombination in mature B cells: a mechanism for altering antibody responses, Science 278 (1997) 298–301.
[22] M. Hikida, H. Ohmori, Rearrangement of λ light chain genes in mature B cells in vitro and in vivo. Function of reexpressed recombination-activating gene (RAG) products, J. Exp. Med. 187 (1998) 795–799.
[23] M. Hikida, Y. Nakayama, Y. Yamashita, Y. Kumazawa, S. Nishikawa, H. Ohmori, Expression of recombination activating genes in germinal center B cells: Involvement of interleukin 7 (IL-7) and the IL-7 receptor, J. Exp. Med. 188 (1998) 365–372.
[24] A. Constantinescu, M.S. Schlissel, Changes in locus-specific V(D)J recombinase activity induced by immunoglobulin gene products during B cell development, J. Exp. Med. 185 (1997) 609–620.
[25] G. Kelsoe, V(D)J hypermutation and receptor revision: coloring outside the lines, Curr. Opin. Immunol. 11 (1999) 70–75.
[26] S. Han, S.R. Dillon, B. Zheng, M. Shimoda, M.S. Schlissel, G. Kelsoe, V(D)J recombinase activity in a subset of germinal center B lymphocytes, Science 278 (1997) 301–305.
[27] C. Giachino, E. Padovan, A. Lanzavecchia, Re-expression of RAG-1 and RAG-2 genes and evidence for secondary rearrangements in human germinal center B lymphocytes, Eur. J. Immunol. 28 (1998) 3506–3513.
[28] H.J. Girschick, A.C. Grammer, T. Nanki, M. Mayo, P.E. Lipsky, RAG1 and RAG2 expression by B cell subsets from human tonsil and peripheral blood, J. Immunol. 166 (2001) 377–386.
[29] N. Meru, A. Jung, I. Baumann, G. Niedobitek, Expression of the recombination-activating genes in extrafollicular lymphocytes but no apparent reinduction in germinal center reactions in human tonsils, Blood 99 (2002) 531–537.
[30] Y. Yanagihara, K. Kajiwara, Y. Basaki, K. Ikizawa, M. Ebisawa, C. Ra, H. Tachimoto, H. Saito, Cultured basophils but not cultured mast cells induce IgE synthesis in B cells after immunologic stimulation, Clin. Exp. Immunol. 111 (1998) 136–143.
[31] Y. Yanagihara, K. Kajiwara, K. Ikizawa, T. Koshio, K. Okumura, C. Ra, Recombinant soluble form of the human high-affinity immunoglobulin E (IgE) receptor inhibits IgE production through its specific binding to IgE-bearing B cells, J. Clin. Invest. 94 (1994) 2162–2165.
[32] K. Kajiwara, C. Ra, Y. Yanagihara, Recombinant soluble form of the high-affinity IgE receptor α subunit and anti-IgE antibody inhibit IgE synthesis by IgE-expressing B cells through distinct pathways, Allergol. Int. 51 (2002) 178–184.
[33] L.S. Lee, H.M. Garnett, Estimation of total DNA in crude extracts of plant leaf tissue using 4′,6-diamidino-2-phenylindole (DAPI) fluorometry, J. Biochem. Biophys. Methods 26 (1993) 249–260.
[34] M. Magari, T. Sawatani, Y. Kawano, M. Cascalho, M. Wabl, N. Kanayama, M. Hikida, H. Ohmori, Contribution of light chain rearrangement in peripheral B cells to the generation of high-affinity antibodies, Eur. J. Immunol. 32 (2002) 957–966.
[35] P. Graber, D. Gretener, S. Herren, J.F. Aubry, G. Elson, J. Poudrier, S. Lecoanet-Henchoz, S. Alouani, C. Losberger, J.Y. Bonnefoy, M.H. Kosco-Vilbois, J.F. Gauchat, The distribution of IL-13 receptor α1 expression on B cells, T cells and monocytes and its regulation by IL-13 and IL-4, Eur. J. Immunol. 28 (1998) 4286–4298.
[36] K. Gee, M. Kozlowski, M. Kryworuchko, F. Diaz-Mitomi, A. Kumar, Differential effect of IL-4 and IL-13 on CD44 expression in the Burkitt's lymphoma B cell line BL30/B95-8 and in Epstein–Barr virus (EBV) transformed human B cells: loss of IL-13 receptors on Burkitt's lymphoma B cells, Cell. Immunol. 211 (2001) 131–142.

Adv. Biophys., Vol.38, pp.45-64 (2004)

THE FUNCTION OF RECQ HELICASE GENE FAMILY (ESPECIALLY BLM) IN DNA RECOMBINATION AND JOINING

HIDEO KANEKO, TOSHIYUKI FUKAO, AND NAOMI KONDO

Department of Pediatrics, Gifu University School of Medicine, 40 Tsukasa-machi, Gifu 500-8705, Japan

RecQ DNA helicase family include 5 helicases. BLM, WRN, RecQ1, RecQ4 and RecQ5. BLM, WRN and RecQ4 are the causative genes for cancer predisposition syndrome; Bloom syndrome (BS), Werner syndrome and Rothmund-Thomson syndrome, respectively. These genes seem to maintain genomic stability (*1-6*). Helicase are molecular motors that convert double-stranded into single-stranded nucleic acids. To catalyze the disruption of hydrogen bonds that hold together duplexes, helicases use energy released from hydrolysis of nucleotide 5'-triphosphates, usually ATP, to move along a strand of nucleic acids and unwind the duplex. The discovery of recQ in *Escherichia coli* in a screen for thymineless death-resistant mutants marked the identification of the first member of a large class of RecQ-related DNA helicase (*7*). Several lines of reports suggest that RecQ can suppress illegitimate recombination, thus helping to maintain genomic stability by preventing the formation of duplexes between imperfectly homologous DNA sequence. Therefore, the impairment of RecQ helicase result in the genomic instability and the development of various types of cancer. In this review we describe the clinical features of BS and the function of *BLM* gene.

Correspondence and requests for materials should be addressed to H.K. (e-mail: hideo@cc.gifu-u.ac.jp)

I. BLOOM SYNDROME

Long-term Study of BS Patients

Bloom syndrome is a rare autosomal recessive genetic disorder characterized by growth deficiency, unusual facies, sun-sensitive telangiectatic erythema, infertility, immunodeficiency and chromosome aberrations, including gaps and rearrangements and a predisposition to diabetes, leukemia and lymphoma. Some of these characteristics including chromosomal instability, immunodeficiency and cancer predisposition are shared with the genome instability syndromes ataxia-telangiectasia (A-T), Nijemegen breakage syndrome (NBS) and Fanconi anemia.

A brother and sister were identified as 96 (HiOk) and 97 (AsOk), respectively, in the Bloom's Syndrome Registry (Table 1) (*8*). Their parent's are first cousins. The diagnosis of BS was verified by a high incidence of chromsome aberrrations and of a high frequency (85±16/cell, 90±18/cell, respectively) of sister chromatid exchanges in lymphocytes. Both of them were undersized at birth. As shown in Fig. 1, they grow below the –2SD line of the growth chart for normal controls.

TABLE 1
Clinical Features of Two Siblings

Features	HiOk	AsOk
Weight at birth	2,100g	2,250g
Height	143.1 cm (21 years old)	144.5 cm (19 years old)
Skin change	Telangiectatic erythema	Telangiectatic erythema
	Brownish pigmentation interspersed with hypopigmented area	Cafe-au-lait spots Hypopigmented area
	Cafe-au-lait spots	Atopic dermatitis
	Atopic dermatitis	
Facies	Malar hypoplasia	Malar hypoplasia
	Mandibular hypoplasia	Mandibular hypoplasia
Intelligence	Within the normal range	Within the normal range
Immune status	Decreased IgM and IgA	Decreased IgM and IgA
	Increased IgE	Increased IgE
	B cell dysfunction	B cell dysfunction
Chromosome	Breakage of chromosome	Breakage of chromosome
	Increased SCEs	Increased SCEs
Other findings	High-pitched voice	Allergic rhinitis
	Mild hepatic dysfunction	Early menopause
	Diabetes mellitus	
	Small testis	

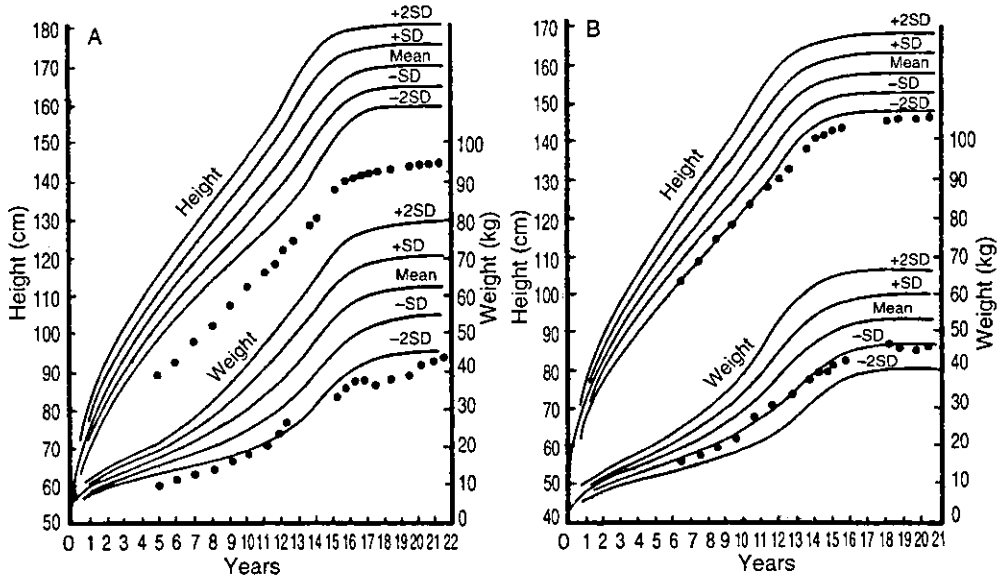

Fig. 1. Growth charts of HiOk and AsOk. The lines represent the mean and SD for Japanese normal controls. A: HiOk, B: AsOk.

Immunodeficiency

They had repeated prolonged middle ear infections and upper respiratory tract infections since the age of 2 years occurring several times per year until about the age of 14 years for HiOk and 12 years for AsOk. The severity and frequency

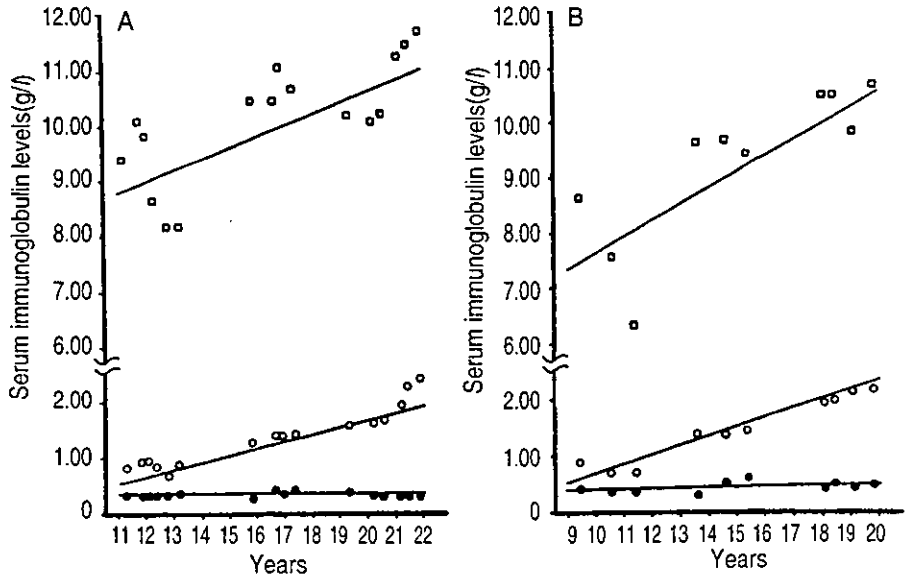

Fig. 2. Time courses of serum immunoglobulin levels in patients with BS. Serum concentration of three major classes of immunoglobulins, IgM (●), IgG (□), and IgA (○), are shown. A:HiOk. The serum concentrations of IgG (g/*l*) and IgA (g/*l*) were significantly correlated with age (years) (for IgG, r=0.73, p<0.005, for IgA, r= 0.94, p< 0.005), but those of IgM (g/*l*) were not correlated with age (years) (r=−0.45). B: AsOk. The serum concentrations of IgG (g/*l*) and IgA (g/*l*) were significantly correlated with age (years) (for IgG, r = 0.80, p<0.01, for IgA, r= 0.97, p< 0.005), but those of IgM (g/*l*) were not correlated with age (years) (r=−0.47). Pearson's correlation test was used.

of infections were lower in AsOk than in HiOk. As the patients grew older, the severity and the frequency of infections gradually decreased. When HiOk was approximately 18 years, the frequency of his middle ear infections decreased to once or twice per several years with sensitivity to therapy after the age of 16 years.

Figure 2 shows the immunological data of both patients with Bloom syndrome at age 11 years and 21 years for HiOk and 9 years and 19 years for AsOk. Serum concentrations of the three major classes of immunoglobulins, IgM, IgG and IgA, were low at age 11 years in HiOk and at 9 years for AsOk, as compared with age-matched control means. However, the magnitude of reduction for each class of immunoglobulin varied. In both patients, serum concentrations of IgM were markedly low, but those of IgG and IgA were only mildly decreased. Neither patient has ever been administered gammaglobulin therapy during the past 14 years. As shown in Fig. 2, the small decrease in serum concentrations of IgG and IgA increased significantly with age, whereas the IgM levels remained low. Serum concentrations of IgG subclasses and specific antibodies of the IgG fraction were not reduced, whereas specific antibodies of IgM fraction were reduced. Neither patient had significantly reduced percentage of circulating $CD3^+$, $CD4^+$, $CD8^+$ or $CD19^+$ cells when compared with controls (*9*).

Diabetes Mellitus

HiOk had mild hepatic dysfunction (GOT, 81 IU/*l* (normal range 7-35 IU/*l*); (GPT, 66 IU/*l* (normal range 7-30 IU/*l*); γ-GTP, 109 IU/*l* (normal range 160-420 IU/*l*)), and both hemoglobin F level was elevated (5.2%; normal range 0-1.2%). oral glucose tolerance test (OGTT) was performed when he was 18 years old and again when HiOk was 21 years old and 0 months old (Fig. 3) (*10,11*). At least in the routine study, diabetic symptoms and diabetic signs such as glucosuria were not detectable until the the second test. AsOk was also examined for OGTT when she was 19 years and 1 month old. After overnight fasting, 75 g of glucose was loaded orally. Blood glucose(BG), plasma immunoreactive insulin(IRI) and C-peptide immunoreactivity (CPR) was measured before and after at 30, 60, 90, 120 and 180 min. Plasma IRI and CPR were measured by double antibody radioimmunoassay. The results of OGTT are shown in Fig. 3. The blood glucose curve indicated the impaired glucose tolerance(IGT) pattern in the male patient' s first test (open circles, solid lines), and indicated the diabetic pattern in his second test (closed circles, solid lines) (National Diabetes Data Group, 1979). In the second test, the plasma IRI level increased from 13.1 to 104.4 μU/ml at 180 min after loading, and the plasma CRP level also increased from 2.0 to 12.0 ng/ml at 120 and 180 min after loading. The ratio of increments of blood insulin to that of blood glucose 30 min after a 75-g glucose load (ΔIRI/ΔBG(30)=insulinogenic index) is used as the most sensitive index to detect the abnormality of early insu-

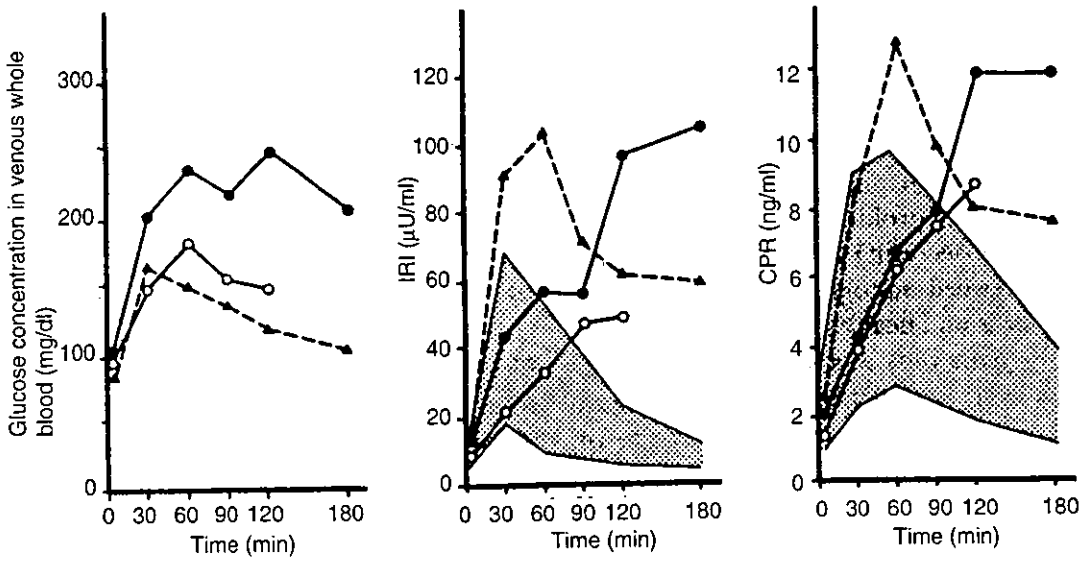

Fig. 3. Oral glucose tolerance test of BS. Blood glucose(BG), plasma immunoreactive insulin (IRI) and C-peptide immunoreactivity (CPR) levels were measured during 75 g oral glucose tolerance test. ○-○: HiOk, at age of 18 years 10 months (the first test); Fasting blood sugar (FBS) value was 90 mg/dl and ΔIRI/ΔBG(30) was 0.22. The blood glucose curve indicated the IGT pattern (the fasting glucose concentration must be below 120 mg/dl; the glucose concentration 2 h after 75g oral glucose challenge must be between 120 and 180 mg/dl). ●-●: HiOk, at age of 21 years 0 months (the second test); FBS was 95mg/dl and ΔIRI/ΔBG(30) was 0.20. The blood glucose curve indicated the diabetic pattern (both the 2-h sample and another sample taken between administration of 75-g glucose dose and 2 h later must be greater than or equal to 180 mg/dl), and plasma IRI and CPR levels markedly increased after glucose loading. ▲-▲: AsOk; at age of 19 years 1 months; FBS was 86 mg/dl and ΔIRI/ΔBG(30) was 0.99. The blood glucose curve indicated the normal pattern (the fasting glucose concentration must be below 100 mg/dl; the glucose concentration 2 h after 75g oral glucose challenge must be between 120 mg/dl). The strippled areas represent the mean±2 S.D. for normal controls.

lin release in diabetes. That is to say, if the ratio of subjects who had mild glucose intolerance was less than 0.5, they would show a higher incidence of worsening to definite diabetes. The subject's ΔIRI/ΔBG(30) was 0.22 in the first and 0.20 in the second test. In contrast, the blood glucose curve of his sister (triangles, dotted lines) was normal, and her ΔIRI/ΔBG(30) was 0.99.

II. LYMPHOMA

B Cell Lymphoma

One of the prominent character of BS is high predisposition to various types of cancer (*12*). After 1 month of treatment with exogenous insulin, HiOk developed B-cell type non-Hodgkin's lymphoma which was sensitive to radiation (30 Gy) in the nasopharyngeal portion. However, after five months of treatment with radiation, the lymphoma relapsed, with widespread abdominal disease which resisted chemotherapy. Twenty-four months after the onset of the lymphoma, he died due to hepatic metastasis (*13,14*).

AsOk complained severe abdominal pain at 25 years old, and we diagnosed her as being in acute abdomen. Colon fiberscope revealed neoplastic changes of the epitherium around the ileum end, and the surgical treatment had been performed. There was a tumor which obstructed intestinal cavity located at 30 cm of oral side from Bauhin's valve, diagnosed as B-cell type non-Hodgkin's lymphoma. She received half dose of the acute lymphoblastic leukemia protocol which is used by our children's cancer study group (9104 standard risk protocol in Tokai Pediatrics Oncology Study Group). In the result, she was medicated the following drugs: vincristine, 0.75 mg/m^2 on days 1, 8, 15, 22, 29, 71, 85, 99, 113, 127, 134, 141; dexamethazone, 6 mg/m^2 on days 1 through 7 and 127 through 133; predonisolone, 30 mg/m^2 on days 8 through 14 and 134 through 140; predonisolone, 15 mg/m^2 on days 15 through 28; L-asparaginase, 5,000 u/m^2 on days 15, 18, 21, 24, 27, 30, 87, 101 and 115; methotrexate 6 mg/m^2, cytarabine 15 mg/m^2 and hydrocortisone 10 mg/m^2 intrathecally on days 22, 29, 36, 43, 72, 86, 100, and 114; daunorubicin 15 mg/m^2 on days 43, 50 and 57; cytarabine, 35 mg/m^2 on days 44 through 47, 51 through 54 and 58 through 61; mercaptopurine, 25 mg/m^2 on days 36 through 63; methotrexate, 1,500 mg/m^2 on days 85, 99 and 113 with leucovorin rescue; cyclophosphamide, 300 mg/m^2 on days 87, 101 and 115; pirarubicine, 15 mg/m^2 on days 127, 134 and 141; enocitabine, 50 mg/m^2 on days 128 through 131, 135 through 138 and 142 through 145. She continues complete remission and free of treatment complications for 5 years after diagnosis.

Phenotype of B Cell Lymphoma Originating from HiOk

Pathological findings showed diffuse, large-cell lymphoma. Surface markers showed typical B cell lineage without the expression of immunoglobulin chains. Also Bcl-2 expression was not detected. Cμ chain and the overexpression of *c-myc* and *p53* genes were not observed. Translocation of *c-myc* and EB virus integration were not detected by Southern blotting.

p53 Mutation of B Cell Lymphoma

p53 mutation is often recognized in B cell lymphoma. The hot spots of *p53* mutations from exon 5 to exon 9 were investigated. No cases showed *p53* mutations in the genomic DNA extracted from neutrophils and lymphoma tissues from the original site. However, a metastatic lymphoma originating from the cecum of HiOk 5 months after radiation therapy showed a reduced length of the *p53* exon 7. DNA sequence analysis revealed 9 bp deletion in exon 7 (Table 2).

III. REPLICATION ERROR

The *BLM* gene encodes a DNA helicase homologue, and DNA helicase constitutes the one of the factors involved in DNA replication. Therefore, dinucleotide

TABLE 2
Mutations in B Cell Lymphoma Originating from BS

	Lymphoma	Lymphoma	Lymphoma		
	Original site (HiOk)	Recurrence site (HiOk)	EB line*2 (HiOk)	Original site (AsOk)	EB line (AsOk)
p53	WT*1	9 bp deletion in exon7 CTCACCATC*4	WT	WT	n.d.*3
Dinucleotide repeat DXS1113	Deletion of one CT repeat and 5 CA repeats	Deletion of one CT repeat and 5 or 6 CA repeats	Deletion of one or 2 CT repeats and 5 or 7 CA repeats	Germline*5	Germline*5
Trinucleotide repeat HUMARA	Deletion of 2 GCA repeats	Deletion of one or 2 GCA repeats	Deletion of 2 GCA repeats	Germline*5	Germline*5

*1WT:Wild type. *2EB line is lane 5 in Fig.5. *3n.d.:not done. *4This mutation causes deletion of 3 amino acids (position 252-254) (Lamb and Crawford, 1986). *5 germline type was judged by detecting identical bands to neutrophil DNA.

and trinucleotide repeat replications on the X chromosome were investigated. Lymphoma DNA from both original and metasatic sites showed the reduced length of repetitive DNA as determined by acrylamide gel electrophoresis. One Epstein-Barr virus(EBV)-transfomed cell derived from HiOk B cells also showed the reduced length of repetitive DNA. DNA sequence analysis revealed 6 or 3 bp deletion in microsatellite DNA HUMARA and 12 or 14 bp deletion in DXS1113, respectively (Table 2).

B cell lymphoma and EB virus transformed cell line derived from AsOk B cells did not show any changes of the length of these repetitive DNA. Microsatellite instability has been detected in a variety of sporadic human tumors. This suggests that a mismatch repair deficiency could strongly accelerate malignant transformation of rapidly expanding cell populations. The function of RecQ helicase, a homologue of BLM, is unclear, although it seems most likely to be one of the factors contributing to postreplication recombinational repair. Although there is no direct evidence that BLM participates in the mismatch repair system, the presence of microsatellite instability in lymphoma cells seems to suggest the involvement of BLM in the mismatch repair system, directly or indirectly.

Dramatic instability of the BS genome has been reported. Groden and German (*15*) reported that 10 of the 33 secondary clones derived from the BS line presented altered hybridization profiles at a tandem-repeat locus and unequal sister-chromatid exchange giving rise to intra-locus mutation was considered the most plausible explanation for the accumulation of the changes detected. The machinery of instability of the BS genome remains to be unclear. It is possible that loss of helicase activity generates abnormal DNA structures during replication which indirectly affect the activity of other DNA-binding proteins or activates repair mechanisms.

IV. IMMUNOGLOBULIN GENE REARRANGEMENT IN BS LYMPHOCYTES

Almost all patients with BS have abnormally low concentrations of one or more of the plasma immunoglobulins and fail to show delayed hypersensitivity. The mechanisms of immunodeficiency remain to be elucidated. The identification of the DNA helicase function of BLM may help us clarify the relationship between lymphocyte differentiation and the complex proteins of DNA repair. The involvement of BLM in DNA repair has not yet been determined. Werner syndrome is characterized by premature aging. The gene that when mutated causes Werner syndrome is *WRN*, which is homologous to *BLM*. However, immunodeficiency is not a characteristic clinical feature of Werner syndrome. *BLM* is preferentially expressed in thymus and testis while *WRN* is ubiquitously expressed with the strong expression in the testis (*16*). The difference in the expression pattern between *BLM* and *WRN* might explain the clinical features of immunodeficiency in BS. In all of the examined hematopoietic cell lines *BLM* expression was detected although the varied amount of expression in each cell lines observed. It was assumed that strong or low expression of *BLM* would appear to correlate with the fast or slow cell growth rate in each cell lines. *BLM* expression of myelomonocyte was detected. Although the function of myelomonocyte in BS has not determined, this might explain that some BS patients with normal serum immunoglobulin also have the susceptibility to infection.

The increased frequency of abnormal T cell rearrangement was observed in the peripheral blood lymphocytes (PBL) of patients with BS compared with control individual. However, the frequency of abnormal rearrangement in PBL of the patients with BS is lower than PBL in ataxia-telangiectasia. In consistent with the previous report (*17-19*) in peripheral B cells from patients with BS the sequences of CDR3 region in VDJ rearrangement examined were in-frame and insertion of N region was also detected. These result suggested that DNA helicase function of BLM is not involved in the VDJ recombination directly. Both T and B cells utilize same machinery of VDJ recombination. BS cells have normal VDJ recombination in immunoglobulin, therefore it is not likely that the increased frequency of abnormal T cell rearrangement in BS is caused by abnormal catalytic function of the recombinase. Another explanation might be abnormal accessibility of the different antigen receptor loci to the recombinase in BS cells. The increased frequency of abnormal T cell rearrangement suggests that BLM is involved in maintenance of DNA stability.

V. *BLM* GENE AND MUTATION

In 1995, the BS gene, *BLM*, was identified and shown to have 4,437 bp that en-

codes 1,417 amino acid peptides with homology to RecQ helicases, a subfamily of DExH box-containing DNA and RNA helicases (*20*) (Fig. 4). It is assumed that the BLM protein plays an important role in the maintenance of genomic stability in somatic cells. In this syndrome, increased spontaneous sister chromatid

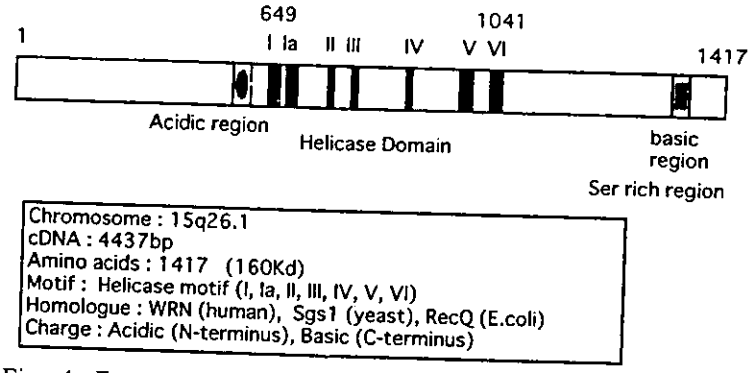

Fig. 4. Feature of BLM protein and functional motif.

TABLE 3
BLM Mutations Identified in Persons with Bloom (*21*)

Identification	Ancestry	Zygosity of the mutation	Nucleotide change	Protein change
Missense mutations				
139(ViKre)	Mixed European	Heterozygous	A2089G	Q627R
31(CaDe)	Dutch	Heterozygous	A2089G	Q627R
40(DoRoe)	Mixed European	Heterozygous	G2776A	C901Y
113(DaDem)	Italian	Homozygous	G3238C	C1055S
Nonsense mutations				
97(AsOk)	Japanese	Homozygous	631delCAA	S186X
112(NaSch)	Mixed European	Heterozygous	A888T	K272X
98(RoMo)	Mixed European	Heterozygous	A1164T	R364X
81(MaGrou)	French Canadian	Homozygous	C1858A	S595X
11(IaTh)	Mixed European	Heterozygous	C2007T	Q645X
61(DoHop)	Mixed European	Homozygous	C2007T	Q645X
NRI(ErBor)	Mixed European	Heterozygous	C2007T	Q645X
NR8(KeSol)	Mixed European	Heterozygous	C2007T	Q645X
51(KeMc)	Mixed European	Homozygous	C2172T	Q700X
Frameshift mutations				
93(YoYa)	Japanese	Homozygous	1610insA	514-1-X
15(MaRo)	Ashkenazi Jewish	Homozygous	2281delATCTGAinsTAGATTC	735-4-X
42(RAFR)	Ashkenazi Jewish	Homozygous	2281delATCTGAinsTAGATTC	735-4-X
107(MyAsa)	Ashkenazi Jewish	Homozygous	2281delATCTGAinsTAGATTC	735-4-X
NR2(CrSpe)	Ashkenazi Jewish	Homozygous	2281delATCTGAinsTAGATTC	735-4-X
126(BrNa)	Ashkenazi Jewish	Heterozygous	2281delATCTGAinsTAGATTC	735-4-X
Exon-skipping mutations				
126(BrNa)	Ashkenazi/ Sepharadic	Heterozygous	Skip exon2	
112(NaSch)	Mixed European	Heterozygous	Skip exon6	
92(VaBia)	Italian	Homozygous	Skip exons 11 and 12	

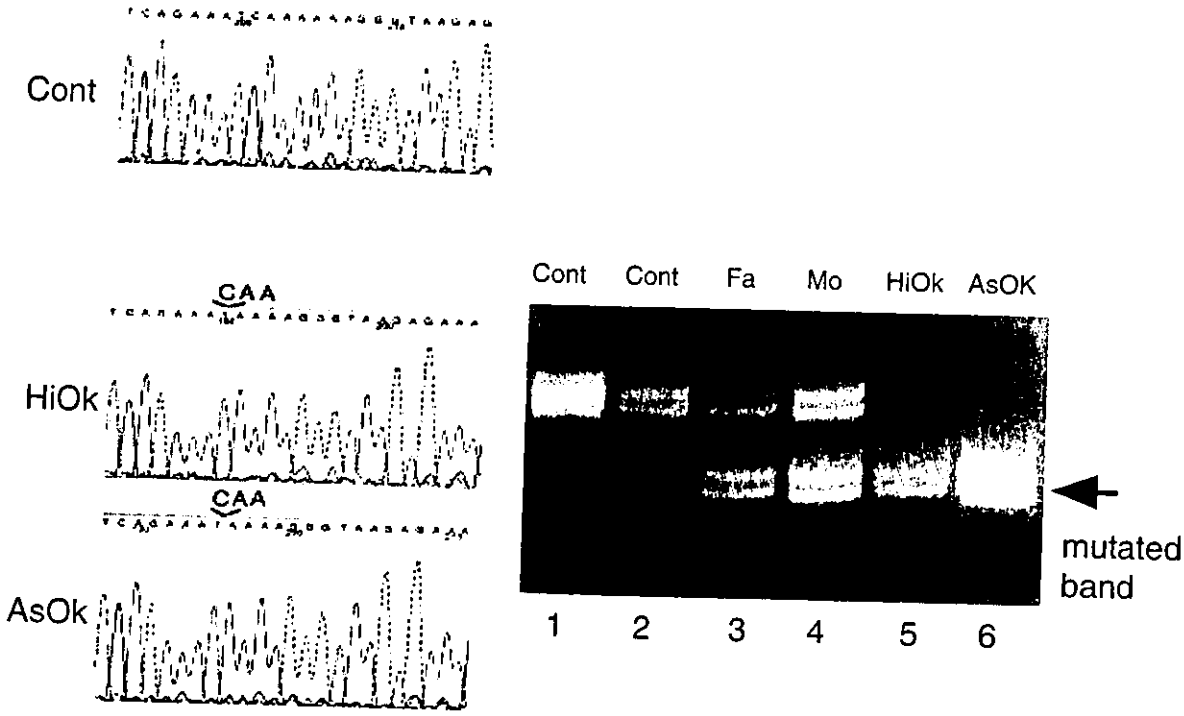

Fig. 5. Mutation of *BLM* gene. *BLM* (514-741) was amplified by PCR and electrophoresised to 12% acrylamide gel for 30 h at 400 V. Lane 1,2: healthy control, lane 3: father, lane 4: mother, lane 5: HiOk, lane 6: AsOk.

exchanges have been observed, and it is thought to be the most malignancy-prone chromosomal disorder. The underlying lesion might be caused by a deficiency in DNA damage repair.

Ellis and German have reported 14 unique mutations in 20 persons with BS out of just the 25 persons examined. Three of the mutations are putative missense substitutions, six are nonsense mutations, two are frameshift mutations, two are exon-skipping mutations and one is a gross deletion detectable by Southern blot analysis (Table 3) (*21*). The relatively high frequency of mutation of the *BLM* gene in the Askenazim has been reported as *blmAsh* which is a 6-bp deletion/7-bp insertion at nucleotide 2,281 of the open reading frame of *BLM* that results in a frameshift and a stop codon at nucleotide 2,292 (*22, 23*). Li *et al.* have reported that *blmAsh* mutation is present in 1 of 107 of this particular Askenazi Jewish population or a carrier frequency of 0.0093. However, in Japanese such a common mutation of *BLM* has not yet been reported. Moreover, it is sometimes difficult to distinguish between BS and other DNA instability syndromes such as, Fanconi or Rothmund-Thomson syndrome based on the clinical manifestations.

In acrylamide gel electrophoresis for 30 hrs, the mobility of PCR amplified *BLM* fragment from HiOk differed from that of healthy control DNA and was similar to that of AsOk DNA (Fig. 5) (*24*). PCR amplified *BLM* fragments from their father and mother DNA showed 2 bands, one with the same mobility

as healthy control DNA and the other with the same mobility as HiOk and AsOk. A 3 bp deletion was detected in the *BLM* sequence from HiOk and AsOK DNA (Fig. 5). This deletion caused generation of a stop codon at amino acid position 186. From the father or mother DNA both deleted and normal-sized *BLM* sequences were obtained.

Recent studies have identified a small increase in the risk of colorectal cancer developing in individuals who are heterozygous for the *blmAsh* allele (*25*). Consistent with this, mice that are heterozygous for *BLM* mutations show enhanced tumor formation when challenged by murine leukemia virus or when crossed with mice that are heterozygous for the APC colon tumor-suppressor gene (*26*). These data indicate that *BLM* heterozygotes other than those with the *blmAsh* allele might be similarly cancer prone.

VI. THE FUNCTIONAL DOMAINS OF BLM

Nuclear Localization Signal in BLM

Based on previously reported manuscripts, although many *BLM* mutations truncate the protein upstream of the helicase domain, *WRN* mutations truncate the protein beyond the helicase domain. These *WRN* mutations probably retain at least DNA helicase activity. Lu *et al.* reported that site-directed mutations that eliminate helicase activity of yeast *Sgs1* can still complement certain *Sgs1* mutants (*27*). It is assumed that differences of disease symptoms caused by *BLM* mutations and *WRN* mutations may be a loss of a function other than the helicase activity (*28*).

By search of BLM amino acids sequence we found putative bipartite nuclear localization signal (NLS) in C-terminal (*29*). Close examination of BLM protein revealed that there are two arms of basic amino acids, those were Arg (R)-Lys (K)-Arg (R)-Lys (K)-Lys (K) (1,334-1,338) and Arg (R)-Ser (S)-Lys (K)-Arg (R)-Arg (R)-Lys (K) (1,344-1,349) in C-terminal (Fig. 6). We prepared the primers for amplifing various length of *BLM*. Each fragments corresponded to putative NLS or helicase domain or previously reported non-sense mutations. The fragments P-9, P-10 and P-11 were produced to corrsponded to the mutations previously reported in the Bloom's Syndrome Registry designations 97, 112 and 93, respectively. The predicted peptides of the frameshit mutation observed in registry No. 15, 42 107 and Nr2 was 739 amino acids residues and located between the fragments of P-7 and P-8. Green Fluorescent Protein (GFP) vector inserted with full coding sequence of BLM was transfected to HeLa cells, which cell lines express BLM abundantly, and GFP was localized in nucleus. The truncated BLM by 1,341 amino acids, which contain only proximal arm of basic amino acids, was not transported to nucleus and retained in cytoplasma. The truncated BLM by 1,356 amino acids, which contain two arms, was transported

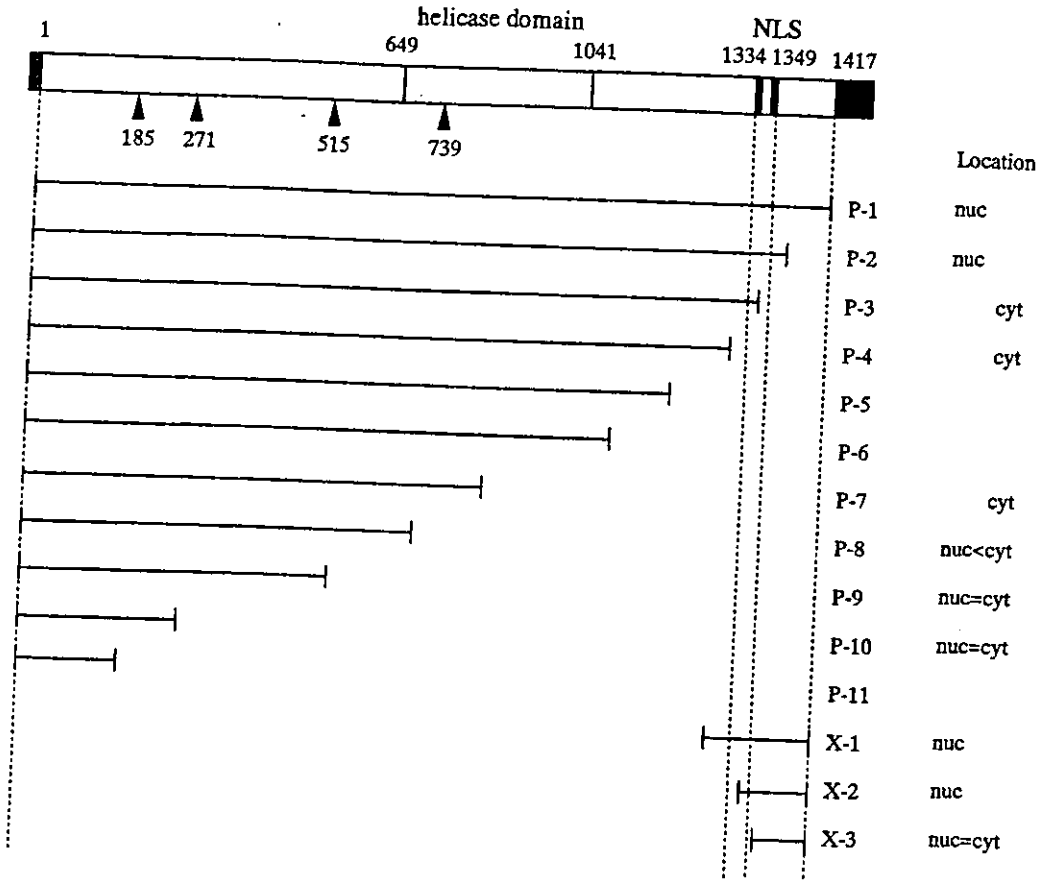

Fig. 6. The summary of the localization of GFP-BLM fusion proteins and the DNA fragments of *BLM* used in this experiments. The number showed the position of amino acids residue in BLM protein. Arrow heads revealed the position of non-sense mutation in previously reported manuscript. nuc: nuclear localization of GFP in all cells observed; cyt: cytplasmic in all cells observed. In those cases were the subcellular location was not exclusively nuclear or cytoplasmic, the results has been given by nuc>cyt, nuc=cyt, or nuc<cyt to indicate the predominant pattern of staining observed in transfected cells.

to nucleus. The GFP vector inserted with DNA fragments which have only two arms of basic amino acids in C-terminal, X-1, was also transported to nucleus. The fragments with only distal arm, X-2, was transported to nucleus. These results suggest that the distal arm of the basic residues in BLM protein is essential for nuclear localization. However, we colud not eliminate the possibility that the proximal arm has the cooperative or additive effect for distal arm. The GFP vector with no insert was diffusely distributed in both cytoplasma and nucleus. Truncated BLM protein corresponding to previously reported *BLM* mutations retained in cytoplasma or both cytoplasma and nucleus. The distribution of both cytoplasma and nucleus observed in the short BLM fragments, those were P-9 to P-11, might reflect the character of GFP itself. In these cases, even if such short BLM fragments would transport to the nucleus, the fragments colud not have the function because of the defective helicase domain.

Full BLM and WRN proteins differ in length by only 15 residues and shared highly conserved helicase domain. Both the N-terminal and C-terminal domains are unique to BLM and WRN, and these unique domains play a role for disease symptoms, respectively. We identified nuclear localization of BLM. In addition, WRN has also the functional NLS in its C-terminal. These results were acceptable, since the helicases catalyses the unwinding of double-strand DNA to provide single-strand templates in nucleus.

In BLM protein, C-terminal region plays a crucial role in the proper function of BLM. In contrast to *WRN*, reported *BLM* mutations is assumed to lose its helicase activity . This is in part affected by the information based on the small number of *BLM* mutations in BS patients. Our observation showed that proper BLM function require both intact helicase activity and intact NLS in C-terminal. Therefore, the mutation of NLS could cause BS as well as the mutations which abolish the helicase activity of BLM.

VII. EXPRESSION OF *BLM* GENE IN PERIPHERAL BLOOD MONONUCLEAR CELLS(PBMCs) AND FETAL TISSUES

Since the BLM protein is relatively large, identification of the gene mutation in *BLM* gene for the diagnosis of BS is laborious. Therefore, for screening the BS patients, the expression of BLM protein and nuclear dot formation were investigated in EBV-transformed lymphoblast cell lines and phytohemagglutinin (PHA)-induced lymphoblastoid cells originating from control and BS patients (*30*). In order to search for the source of the BLM protein expression, we investigated the *BLM* gene expression. As previously described, the *BLM* gene was expressed in freshly prepared PBMCs although EBV-transformed B cell line expressed the *BLM* gene strongly. PBMCs stimulated with PHA slightly induced the *BLM* gene. *BLM* gene expression in human fetal tissues was investigated by Northren blotting. The fetal kidney, heart and liver scarecely expressed the *BLM* gene. In the 7-week brain *BLM* gene expression was strongly detected in constrast to the adult brain. As fetal neurons proliferated, the *BLM* gene might be expressed. In a whole embryo, *BLM* gene is strongly expressed in 6 weeks.

VIII. EXPRESSION OF BLM PROTEIN IN HEMATOPOIETIC CELL LINES AND PHA-STIMULATED PBMCs

Next, we investigated the BLM protein expression in various hematopoietic cell lines using polyclonal BLM antibodies. A 160-kd protein was detected in control EBV-transformed cell lines. By immunoblotting, the 160-kd band was strongly detected in haematopoietic leukemic cell lines including B cells, T cells and myelomonocytes. In EBV transformed-lymphoblast cell line, the BLM pro-

tein was detected. We examined 10 more control cell lines and the BLM protein was clearly detected in all of these cell lines when 30 μg of protein was loaded. However, in EB cell lines obtained from BS patients (3403F, H9152, AsOK) the BLM protein was not detected. In freshly isolated PBMCs, the BLM protein was scarcely detected. As the amount of the BLM protein was very low in quiescent PBMCs, we predicted that this might also be in part reflected in *BLM* mRNA levels. However, in PHA-stimulated lymphoblasts BLM protein was significantly induced. The induction of BLM protein started at day 2 after stimulation and continued until day 5. However, PHA-stimulated lymphoblasts from AsOK showed no induction of the BLM protein.

IX. NUCLEAR DOT FORMATION OF BLM PROTEIN

Next, immunohistochemical analysis of the BLM protein was performed (Fig. 7). In the control EB cell line, nuclear dot formation was observed. When stimulated with PHA, some PBMCs exhibited nuclear dots in the nucleus. Other cells did not exhibit nuclear dots, suggesting that the nuclear dots formation depends on the cell cycle of each cell. However, in PHA-stimulated PBMCs obtained from BS no dots formation was observed. PBMCs from AsOk showed comparable levels of ^{3}H-thymidine incorporation (51,337 cpm) to PBMCs from healthy control (37,700-62,400 cpm) indicating the normal activation of peripheral T cells in BS patient.

X. PROTEINS ASSOCIATED WITH BLM

BLM physically and functionally interacts with an array of proteins whose primary role is the maintenance of genome integrity. It has been reported that BLM is associated with the other proteins, those are p53, Top3α and SUMO-1 (Fig. 8) (*31-35*). We have found that BLM formed dots/rod-like structures associated

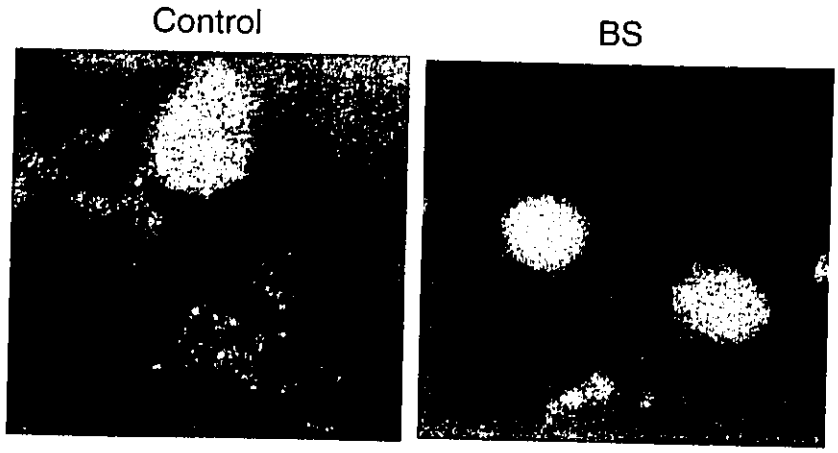

Fig. 7 Nuclear dot formation of BLM in PHA-stimulated PBMCs from control (left) and BS patient (AsOk) (right).

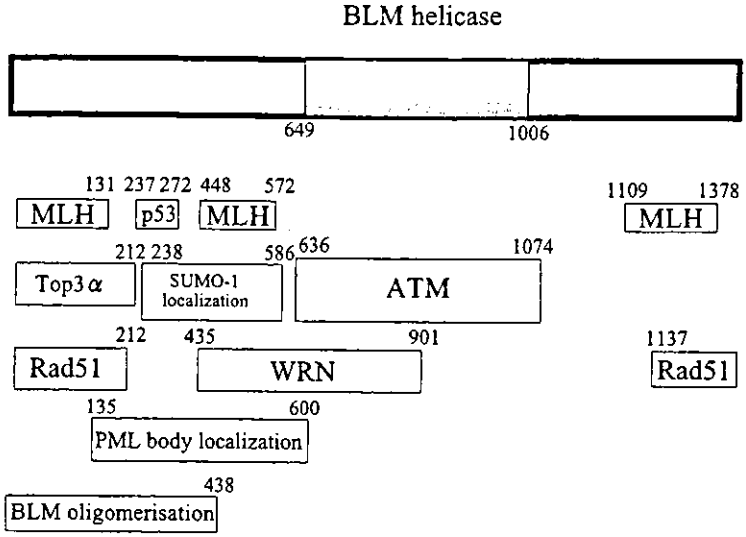

Fig. 8 Interacting proteins with BLM. Regions of the protein where interactions with other proteins have been identified, are shown.

with SUMO-1 in the nucleus. The region from amino acids 238 to 586 of BLM is required for the formation of dots/rod-like structures associated with SUMO-1. Biological meaning of the formation of dots like structure which are associated with SUMO-1 is unclear at present.

XI. BLM INTERACTS DIRECTLY WITH ATM

The phenotype observed in BS suggests that BLM plays a role in recognizing abnormal structures in DNA and suppressing recombinational events that lead to genomic instability. To understand more fully the role of BLM in maintaining genomic stability, we initially employed the yeast two-hybrid system to identify proteins that interact with and influence the function of BLM. Sequence analysis of two strongly positive clones (3F3 and 3C5) identified a 5.5-kb fragment from the C-terminus of *ATM* (ataxia-telangiectasia-mutated) cDNA (3F3) and *BLM* cDNA (3C5). Self-interaction is in keeping with results showing that BLM forms hexameric ring structures (*36*).

BLM bound to GST (glutathion *S*-transferase)-ATM-1 (amino acid residues 1-257), GST-ATM-10 (residues 2,427-2,641), and GST-ATM-12 (residues 2,682-3,012) in reactions without ethidium bromide. However, when this compound was included, GST-ATM-1 and GST-ATM-12 were found to bind equally well to BLM, but there was reduced interaction with GST-ATM-10. Binding of BLM to GST-ATM-10-12, which contains the kinase domain of ATM, is consistent with this protein being a substrate for ATM kinase. Binding studies with ^{35}S-labeled BLM revealed that the smallest region of overlap was a sequence of ~24 nucleotides, which corresponds to amino acids 82-89. Mapping the region of interaction in BLM was carried out using four overlapping GST fusions (GST

1-4, numbered from the N-terminal end). Binding of GST-BLM-3 amino acid residues 636-1074 to ^{35}S-labeled full-length ATM was observed.

Correction of SCE and Radiosensitivity in BS Cells

A major characteristic of A-T cells is extreme sensitivity to ionizing radiation. Since we had shown that BLM and ATM interact, it was possible that this interaction might influence the radiation response and that loss of BLM in BS cells might exacerbate this response. It is clear from the results that HG1525 and HG2703 cells are intermediate between control and A-T cells in radiosensitivity. These two cell lines are characteristic of BS cells with elevated SCE in the unirradiated state, HG1525 (75.7 SCE/46 chromosomes) and HG2703 (82.5 SCE/46 chromosomes) as compared with three to seven in controls. To test the specificity of these observations, we stably transfected BS cells with an EBV-based vector expressing full-length BLM under the control of an inducible metallothionein promoter (HG1525/BLM). Incubation of transfected cells with $CdCl_2$ led to an induction of BLM to a level comparable with that expressed in control cells. This level of expression enhanced the radioresistance of BS cells to that in controls. Radiation-induced chromosome aberrations in BS cells were also reduced after transfection with full-length *BLM* cDNA from 2.0 to 1.35 induced chromosome aberrations/metaphase. The induced chromosome aberration value for controls is 0.92 ± 0.11, whereas that for A-T is 3.03 ± 0.09.

Mitosis-associated Phosphorylation of BLM Is ATM-dependent, and ATM Phosphorylates BLM at Two Sites

Since BLM is hyperphosphorylated in mitosis (*37*), we determined whether this phosphorylation was ATM-dependent and what sites were involved. Cells were blocked in G2/M with the microtubule-stabilizing agent, nocodazole, released and harvested 1 h later, and immunoblotting for BLM was carried out. The majority of BLM exists in a hyperphosphorylated form (retarded species) for control cells at 1 h after release from nocodazole (69% G2/M cells). The ratio of phosphorylated to unphosphorylated BLM was ~3 for the control cell line and 2 for a second control. On the other hand, in three A-T cell lines examined, the greatest proportion of BLM was in the hypophosphorylated form at 1 h after release with the ratio of the two forms ranging from 0.2 to 0.8 (65-73% G2/M cells). Since we showed that BLM interacts directly with ATM, we determined whether BLM was a substrate for ATM kinase. To address this, we employed the four overlapping GST-BLM fusion proteins (described above) as substrates for immunoprecipitated ATM. Only the GST-BLM-1 (N-terminal) fragment is phosphorylated by ATM kinase. When immunoprecipitates from an A-T cell line, L3, were used, no kinase activity was observed. Based on consensus sequences described by Kim *et al.* (38), two potential phosphorylation sites (TQ 99-101; TQ 122-123) were

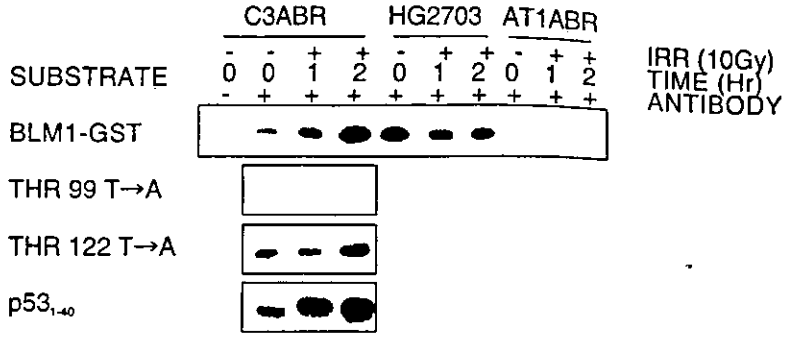

Fig. 9 BLM is a substrate for ATM kinase. Phosphorylation of GST-BLM fusion proteins. ATM was immunoprecipitated from control extracts, and ATM kinase activity was determined using the GST-BLM fusion proteins 1-4. Mutation of the two potential ATM kinase sites in GST-BLM1 site 1. 98-ETQR-101 was mutated to EAQR by mutating nucleotide 369 (an A to a G). In site 2, 121-TTQN-124 was mutated to TAQN by mutating nucleotide 437 (an A to a G). Radiation induced phosphorylation of BLM1 fragments. Extracts were prepared from C3ABR (control), HG2703 (BS), and AT1ABR (A-T) cells at 0, 1, and 2 h post-irradiation (10 Gy), and ATM kinase activity was determined. Activity was also determined using the two mutated fragments (Thr-99 Thr→Ala and Thr-122 Thr→Ala) and $p53_{1-40}$.

identified in the BLM N-terminal peptide for ATM kinase. A chromatographically purified N-terminal fragment of BLM (amino acids 1-200) was also efficiently phosphorylated by ATM. Mutation of Thr-99 to glycine resulted in a significant reduction in phosphorylation of the thrombin-cleaved GST fusion protein by ATM, indicating that this was a major site for ATM kinase *in vitro*. Residual phosphorylation suggests that Thr-122 is also phosphorylated to a lesser extent. When cells were exposed to radiation, there was an enhancement of ATM kinase activity over a 2-h incubation period using the GST-BLM fragment as substrate (Fig. 9). However, as expected, when a fragment with mutated Thr-99 was employed, radiation did not lead to phosphorylation.

Functional Significance of Phosphorylation Sites

A low basal level of phosphorylation on Thr-99 of BLM, which increased with increasing radiation dose. It is evident that this is ATM-dependent since the response is much reduced in A-T cells. Immunoprecipitation with anti-BLM antibody showed normal levels of BLM in control and A-T cells. As a further test of functional significance, we employed Thr-99 and Thr-122 mutant forms to establish stable cell lines. Expression of either the Thr-99 or Thr-122 mutants in BS cells failed to correct radiosensitivity, whereas normal full-length BLM cDNA restored survival to normal levels. However, as for full-length BLM, both mutants reduced SCE levels to those observed in control cells, providing evidence for a dissociation of SCE and DNA damage-induced aberrations. When introduced into control cells, full-length BLM did not alter the phenotype, but the Thr-99 and Thr-122 mutants sensitized these cells to radiation to an extent inter-

mediate between control and A-T and caused a significant elevation in the number of radiation-induced chromosome aberrations. These data suggest that ATM and BLM function together in recognizing abnormal DNA structures by direct interaction and that these phosphorylation sites in BLM are important for radiosensitivity status but not for SCE frequency. We made ATM and BLM double knockout cells from DT40 cells (*39*). Double knockout cells dose not exacerbate either phenotypes of $ATM^{-/-}$ or $BLM^{-/-}$. However, the more extreme radiosensitivity seen in $ATM^{-/-}$ and the elevated SCE seen in $BLM^{-/-}$ cells were retained in the double mutants. These results suggest that ATM and BLM have largely distinct roles in recognizing different forms of damage in DNA, but are also compatible with partially overlapping functions in recognizing breaks in radiation-damaged DNA.

XII. KNOCKOUT MICE

It has been reported that the establishment of BLM knockout mice in a few laboratories. The features of BLM knockout mice showed the striking differences since the BLM gene in the mouse was disrupted by the different strategies (*40, 41*).

However, unlike human BS, three of the knockout mice showed embryonic lethality. Only one developed to maturity. Chester *et al.* reported that mouse homozygous for a targeted mutation in murine BLM are developmentally delayed and die by embryonic day 13.5. Cultured murine $BLM^{-/-}$ fibroblasts showed that high numbers of SCEs. The growth retardation in mutant embryos can be accounted for a wave of increased apoptosis. The mutant embryos do not survive past day 13.5, and at this time exhibit severe anemia.

Luo *et al.* reported the mice homozygous with *BLM* allele with duplicated exon 3, which do not express detectable BLM protein. The cell lines from these mice show elevations in the rates of mitotic recombination. The mouse is viable although by the age of 20 months, nearly a third of them had developed cancer, mainly lymphomas and carcinomas. Luo *et al.* demonstrate that the increased rate of loss of heterozygosity (LOH) resulting from mitotic recombination *in vivo* constitutes the underlying mechanism causing tumour susceptibility in these mice.

SUMMARY

Bloom syndrome is a rare autosomal recessive genetic disorder characterized by lupus-like erythematous telangiectasias of the face, sun sensitivity, stunted growth, and immunodeficiency. Chromosome instability syndromes have a common feature, being associated at high frequency with neoplasia. BS is con-